Research Article

Coexistence Performance of High-Altitude Platform and Terrestrial Systems Using Gigabit Communication Links to Serve Specialist Users

Z. Peng and D. Grace

Communication Research Group, Department of Electronics, University of York, Heslington, York YO10 5DD, UK

Correspondence should be addressed to Z. Peng, kenji0233@hotmail.com

This paper presents three feasible methods to serve specialist users within a service area of up to 150 km diameter by using spot-beam gigabit wireless communication links from high-altitude platforms (HAPs). A single HAP serving multiple spot beams coexists with terrestrial systems, all sharing a common frequency band. The schemes provided in the paper are used to adjust the pointing direction of aperture antennas operating in the mm-wave bands, such that the peak carrier to interference plus noise ratio (CINR) is delivered directly toward the location of the specialist users; the schemes include the small step size scheme, half distance scheme, and beam switch scheme. The pointing process is controlled iteratively using the mean distance between the peak CINR locations and user positions. The paper shows that both the small step size and half distance schemes significantly enhance the CINR at the user, but performance is further improved if beams with adverse performance below a specific threshold are switched off, or are assigned another channel.

1. INTRODUCTION

HDTV is now a hot topic in the consumer electronic space, and while content can be readily delivered from the studio and other specific locations, it is still quite difficult to deliver live content at short notice from outside broadcast locations. An uncompressed HDTV signal is preferred by broadcasters for prebroadcast content since compression introduces excessive delay, and if the compression is lossy, it is liable to introduce progressive degradation of the signal. The data rate required to deliver an uncompressed video stream is up to 3.0 Gbps [1], which is substantially higher than the speed of 10–30 Mbps to transmit 1080i compressed signal [2]. Currently, it is quite difficult to deliver HDTV prebroadcast content due to the high data rates involved. Using gigabit links from a high-altitude platform (HAP) will provide one possible solution to overcome these delivery prebroadcast material problems, at least for the lower resolution formats of HDTV.

High-altitude platforms (HAPs) are being developed as a possible technology to realize the increasing demands

for multimedia applications instead of using traditional landlines or terrestrial systems. HAPs are either aircrafts or airships operating at an altitude of nearly 17–22 km [3, 4]. They show a capability of servicing a large coverage area, which can include places often inaccessible by normal communication systems. They can also provide broadband by sharing the frequency spectrum and offer the potential of a higher spectrally efficiency.

The purpose of this paper is to examine the HAP highly directional spot-beam downlinks when sharing the same frequency band with terrestrial point-to-point system. The scenario is designed to serve the specialist users located in a 300 km diameter service area. The location of the specialist users is called points of interest (POI) in the following sections which are randomized in each scenario. The paper examines three schemes to adjust the pointing direction of the multiple aperture-based antennas with the aim of providing the highest CINR value at the specialist user. A frequency of 28 GHz is selected for use in order to provide the necessary beamwidth and ensure antennas can be made small enough to use for practical application,
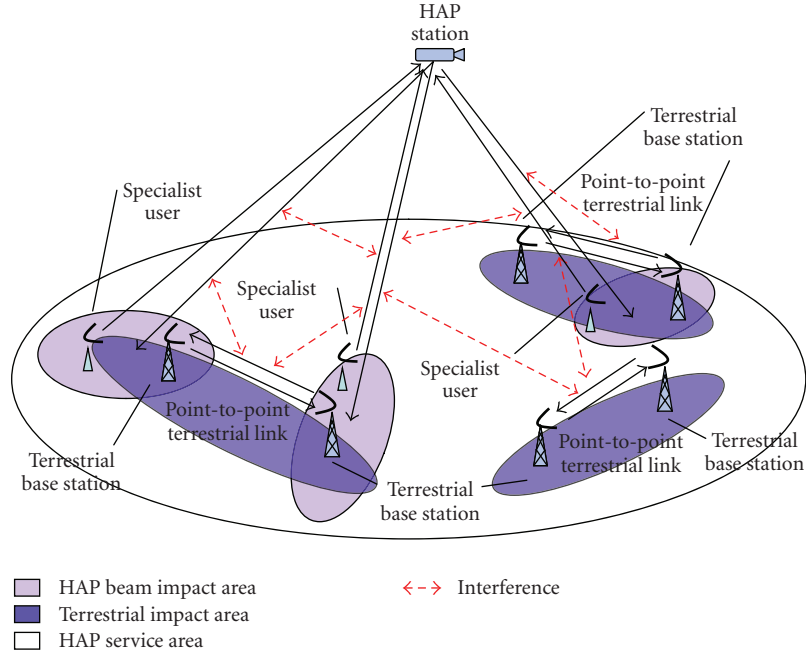
FIGURE 1: The single HAP with multiple-directional antennas and terrestrial point-to-point links.

for example, for an HDTV specialist user discussed above. Normally, specialist users are served by satellites, which due to link budget constraints will supply links with data rates of much less than 1 Gbps. Moreover, the users themselves operate outside broadcast equipment, vans, and so forth, which require a steerable dish to provide the links. Given these disadvantages, high-altitude platforms (HAPs) provide a practical alternative with the ability to provide both high data rate signals, due to the 69 dB link budget advantage compared to GEO satellites and the necessary flexibility to immediately respond to the demands from the users, while serving a wide area of coverage.

This paper is composed of three sections: we will discuss the system scenario in the following section which will discuss the three schemes: the short step size scheme, the half distance step size scheme, and the beam switch scheme; system performance will be deliberated after each scheme; we also draw conclusions at the end of this paper.

2. SYSTEM SCENARIO

The International Telecommunications Union (ITU) has provided a regulatory framework for HAPs to provide 3G services at 2 GHz and also in the millimeter-wave bands around 28/31 and 47/48 GHz [3–7]. Since high-altitude platforms will operate in the stratosphere, it gives them a significant link budget advantage compared with satellites, and a wider coverage area than terrestrial systems. In our scenario, the HAP station and terrestrial stations will share a same frequency band of 28 GHz. We examine the feasibility of such an approach because in this band, HAPs will have to share this band with terrestrial systems. Moreover, the

highly directional antenna characteristics of both terrestrial users and HAP specialist users should mean that coexistence is feasible, providing access to the spectrum is appropriately controlled.

Thus, the scenario consists of an HAP capable of delivering multiple spot beams point-to-point links alongside multiple terrestrial point-to-point links located inside the HAP service area. To provide the greatest flexibility, we examine the situation, where the HAP station is located away from the center of the service area, which is 60–300 km in diameter. The terrestrial stations are randomly located inside the service area as shown in Figure 1. For the HAP station, we consider multiple-directional aperture antennas (we use 20 antennas in this scenario) operated from a single aircraft, pointing at random points of interest within the service area. For the point-to-point terrestrial link, the two-terrestrial stations point directly to each other using highly-directional antennas, as point-to-point communications links. These links share the same frequency as the HAP. HAP users are assumed to point their directional antennas directly toward the HAP.

Unlike the papers that have considered the potential coverage area served, we are more concerned with the interference to the ground user from both the terrestrial stations and other antennas on the HAP which serve other users. The interference due to coexistence of both systems using the same frequency band is evaluated in order to determine the mutual impact on the systems. To evaluate both impacts, we first have to calculate two important system parameters, the carrier to noise ratio (CNR) and the carrier to interference plus noise ratio (CINR). The performance of this scheme relies on the fact that the CNR and CINR can be

evaluated at different points on the service area. The CINR of both HAP and terrestrial test users can be calculated as in [8–10]:

$$\text{CINR} = \frac{C}{N_F + I}$$

$$= \frac{P_{Hm}A_{Hm}(\varphi_m)A_U(\theta_m)(\lambda/4\pi d_m)^2}{N_F + \sum_{j=1}^{N} P_{Hi-j}A_{Hi-j}(\varphi_j)A_U(\theta_j)(\lambda/4\pi d_m)^2}, \quad (1)$$

while the CNR can be calculated as in [5–7]:

$$\text{CNR} = \frac{C}{N_F} = \frac{P_{Hm}A_{Hm}(\varphi_m)A_U(\theta_m)(\lambda/4\pi d_m)^2}{N_F}, \quad (2)$$

where N_F is the thermal noise floor. P_{Hm} and P_{Hi} are the transmit power from one antenna beam of the HAP, and jth interfering antenna beam, respectively. $A_{Hm}(\varphi_m)$ and $A_{Hi}(\varphi_i)$ are the transmit gain of base station antenna, and jth interfering HAP antennas at an angle ϕ_m away from boresight. $A_U(\theta_m)$ and $A_U(\theta_i)$ are the receive gain of the user antenna for the main, and jth interfering at an angle θ_m away from its boresight. $\lambda/4\pi d_m$ is the path loss from the main antenna beam, and the jth interfering antenna beam. λ is the wavelength, and d_m is the distance between the HAP station and the ground user. Techniques for producing elliptic beam antennas for optimizing geographical coverage are also discussed in [11, 12].

2.1. Antenna gain factor

The HAP and user antenna discussed in Section 2 can be described in terms of the main lobe and sidelobes, producing the following equations, respectively, [4–7],

$$\begin{aligned} A_H(\varphi) &= G_T(\max[\cos^{n_H}(\varphi), s_f]), \\ A_U(\theta) &= G_R(\max[\cos^{n_U}(\theta), s_f]), \end{aligned} \quad (3)$$

where G_T is the boresight gain of the HAP, G_R is the boresight gain of the user antenna, and s_f is the main lobe associated with the sidelobe. $G = \eta \cdot (\pi \cdot k/\alpha)^2$, where η is the antenna efficiency, k is a factor that depends on the shape of the reflector and the method of illumination, α is the half power beamwidth. n_H and n_U control the rate of the main beam power roll-off of the HAP antenna and the user antenna, respectively. We adopt a circularly symmetric beam in order to simplify the calculation and assume that it can point in any direction to serve users in the service area. The transmit power from all users/antenna beams of HAP is assumed to be identical.

2.2. Antenna sidelobe analysis

In our scenario, we do not apply a flat sidelobe model, for example, −30 dB as used in other papers since the absolute sidelobe level is more important for this case due to the high gain of the main lobe. Here, we use the model suggested by ITU-R to more accuracy in the region of the main lobe and for sidelobe [8]. Thus, the possible pattern commencing
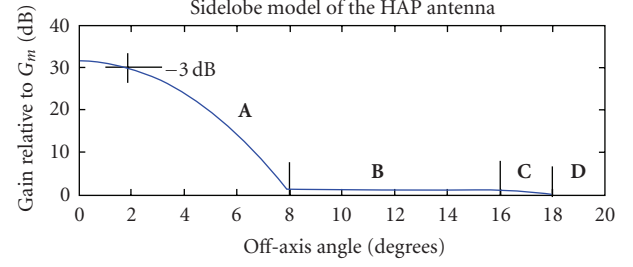

FIGURE 2: Radiation pattern envelope function.

at the boresight of the main lobe can be divided into five regions. These are illustrated in Figure 2.

The four regions below the −3 dB point can be described as follows [11]:

(A)

$$G(\Psi) = G_m - 3\left(\frac{\Psi}{\Psi_0}\right)^2 \quad (4)$$

for $\Psi_0 \leq \Psi \leq 2.58\Psi_0$,

(B)

$$G(\Psi) = G_m + L_s \quad (5)$$

for $2.58\Psi_0 \leq \Psi \leq 6.32\Psi_0$,

(C)

$$G(\Psi) = G_m + L_s + 20 - 20\log\left(\frac{\Psi}{\Psi_0}\right) \quad (6)$$

for $6.32\Psi_0 \leq \Psi \leq \Psi_1$,

(D)

$$G(\Psi) = 0 \quad (7)$$

for $\Psi_1 \leq \Psi$.

Where $G(\Psi)$ represents the gain at the angle (Ψ) from the boresight (dBi); G_m is the maximum gain in the main lobe (dBi); Ψ_0 is the one-half 3 dB beamwidth in the plane of interest (3 dB below G_m) (degrees); Ψ_1 is the value of (Ψ) when $G(\Psi)$ in (6) is equal to 0 dBi; L_s is the required near-in-sidelobe level (dB) relative to the peak gain. This model is not difficult to apply when operating with a circular beam.

2.3. System parameters

With this scenario, we consider the effect of the antenna beamwidth on performance by setting the beamwidth of both HAP and terrestrial station antennas to 5 degrees. The important system parameters for the HAP, terrestrial station, and test users are shown in Table 1.

3. LOCATION OF PEAK RECEIVED POWER CALCULATION

Figure 3 shows the relationship between the peak received power location and the aiming point of the HAP antenna. Given that these highly-directional antennas on the HAP are not likely to point toward the subplatform point, the
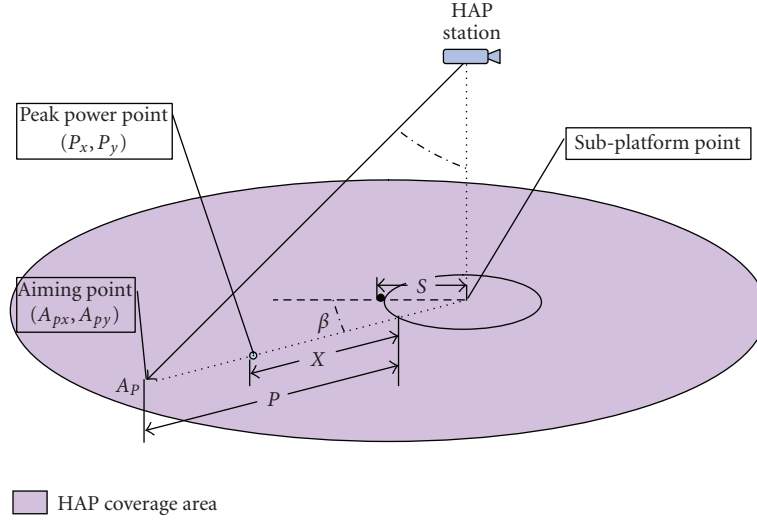
FIGURE 3: Peak receiving point and aiming point from different directional antennas of a single HAP.

TABLE 1: System parameters.

Parameter	HAP base station	Terrestrial point-to-point terminal	Specialist user
Coverage radius	150 km	N/A	N/A
Transmitter height	17 km	10 m	10 m
Antenna gain	31.4 dB	31.4 dB	45.4 dB
Roll off rate	727.9	727.9	18204
Antenna beamwidth	5 degrees	5 degrees	1 degree
Frequency		28 GHz	
Side lobe level		specified	
Noise power		-103.8 dBW	

peak received power point deviates from the aiming point due to the path loss gradient behavior between the SPP and the POI. This deviation is a very important factor that concerns us because specialist users will require good received power performance. The more the boresight of the antenna deviates from the perpendicular line, the further the peak received power point deviates from the aiming point. Given this mutual interaction between the peak received power point and the aiming point of antenna, we can calculate the optimum aiming point of a directional antenna from the HAP by specifying the peak received power location first as required by the individual specialist ground users. More information in detail will be given to show how the peak received power location and/or aiming points can be calculated.

In our scenario, the HAP is assumed not to be at the center of the service area, so it means the HAP spacing radius, defined as the distance from the center of the service area to the subplatform point (SPP) is nonzero (here assumed to equal 10 km). The peak received power location will be on the same line with the aiming point, so we can use the same coordinate ratio (e.g., assuming a set of x coordinates, then $x1/x2 = x3/x4$) to calculate the unknown parameter (aiming point or peak CNR point).

Changing the beamwidth of the HAP antenna will cause the location of the peak received power also to move, as can a change in the spacing radius. It is possible to derive the location of the peak received power from the HAP taking into account spacing radius, antenna roll-off, and pointing offset. Assuming that the center of the service area and the antenna aiming point are along the X-axis, the location of the peak received power point will also move along the X-axis. To calculate the location of peak received power as a function of HAP location and HAP antenna pointing location, we can differentiate the carrier part of (1) with respect to user location and set it equal to zero. Equation (1) is differentiated as [6]

$$\frac{d(\text{Carrier})}{dx} = \frac{d[P_{Hm}A_{Hm}(\varphi_m)A_U(\theta_m)(\lambda/4\pi d_m)^2]}{dx} = 0.$$

(8)

Only $\cos^{n_H}(\phi)$ and d_m^2 are related to the user location, so we may write [6] the following:

$$\frac{d(\text{Carrier})}{dx} = \frac{d[\cos^{n_H}(\varphi)(1/d_m)^2]}{dx} = 0,$$

(9)

where [6]

$$\cos(\varphi) = \frac{[(S-X)^2 + H^2] + [(S-P)^2 + H^2] - (X-P)^2}{2\sqrt{(S-X)^2 + H^2} \cdot \sqrt{(S-P)^2 + H^2}},$$
(10)

$$d_m = \sqrt{(S-X)^2 + H^2},$$
(11)

where P is the distance between antenna aiming point and the center of the service area, X is the distance between peak received power point and the center of the service area, S is the HAP spacing radius, and H is the height of the HAP. Finally, the following equation is derived [6]:

$$2(P-S)X^2 + [4S(S-P) + H^2(n_H + 2)]X \\ - 2S(S^2 + H^2 - S\cdot P) - n_H \cdot H^2 \cdot P = 0.$$
(12)

This quadratic equation (1) can be solved as a function of the above parameters to yield the location of the peak received power on the axis as follows [6]:

$$X = \frac{-B \pm \sqrt{B^2 - 4AC}}{2A},$$
(13)

where

$$A = 2(P-S),$$
$$B = 4S(S-P) + H^2(n_H + 2),$$
$$C = -2S(S^2 + H^2 - S\cdot P) - n_H \cdot H^2 \cdot P.$$
(14)

Now, we can generalize the result for the required aiming point (A_{px}, A_{py}) on the service area in order for the peak received power to be at point (p_x, p_y).

X the ground distance between the peak received power point and the center of the service area can be derived from (10), (12), (13), and

$$X = \frac{p_X - S}{\cos \beta} - S,$$
(15)

where

$$\beta = \arctan\left(\frac{p_Y}{p_X - S}\right).$$
(16)

Thus, we have

$$P = \frac{2SX^2 - 4S^2X - H^2(n_H + 2)\cdot X + 2S^3 - 2SH^2}{2X^2 - 4SX - 2S^2 - n_H \cdot H^2},$$
(17)

where (A_{px}, A_{py}) is the location of the aiming point. This calculation is based on the proof [6] that the peak received power is exactly on the line between the antenna aiming point and the HAP subplatform point. As we know the method to calculate the peak received power point, we could alternatively derive the location of aiming point of the antenna by using a given peak received power point. The equations are shown as

$$A_{px} = (P-S)\cos\beta + S,$$
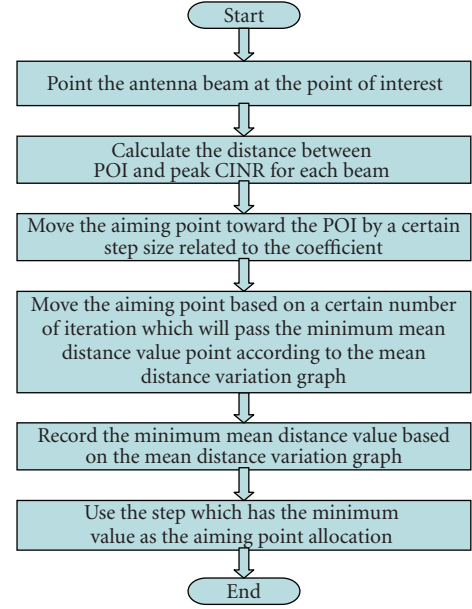$$A_{py} = (P-S)\sin\beta.$$
(18)

FIGURE 4: Flowchart of small step size scheme.

Given this mutual relationship between the two points, we can also extend this analysis to additionally calculate the location of the peak received power point, given a specific aiming point.

4. CONTROLLING CINR BEHAVIOR

The HAP station in this scenario is aimed to serve the specialist users by using several directional antennas identical in number to the specialist users. Each antenna will directly point at a certain location which can give the respective user the peak CNR that we call the point of interest (POI). However, as the number of beams increases, the peak CINR point of the antenna will not coincide with the POI due to the interference from other antenna beams and the terrestrial systems. The purpose of the schemes developed here is to move the peak CINR to the point of interest, while coping with the mutual interaction caused by the interference.

4.1. Scheme I: small step size scheme

From an antenna beam perspective, the aiming point determines the level of the CINR, so that moving the aiming point is the way to modify the location of the peak CINR. However, applying the scheme by modifying only the pointing of one antenna will impact on the other CINR levels seen by other users inside the service area. In order to mitigate such a problem, we apply the scheme to every HAP antenna beam simultaneously with the aim of reducing the mutual interference.

As the distance between the point of interest and the peak CINR point of each antenna beam is different, we are unable to ensure that peak CINR and POI coincide after the iteration, so instead we apply the algorithm repeatedly. Concerned with the distance between peak CINR and POI
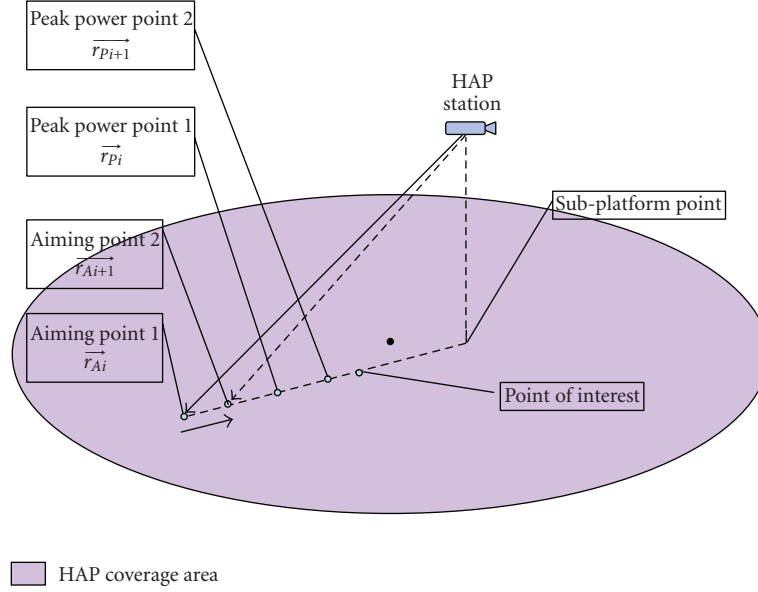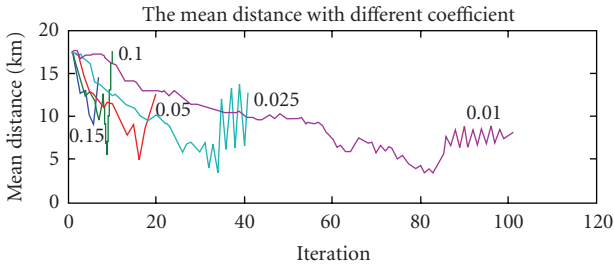
FIGURE 5: The small step scheme description.

FIGURE 6: The mean distance between peak CINR and POI with different coefficients in a small step scheme.

points, we move each aiming point of the beam in the same ratio. We can see how the small step scheme works in Figure 4.

The small step size scheme moves the aiming point based on a very short distance each time according to the flowchart shown in Figure 4. The step size can be specified in terms of the distance between peak CINR point and the POI with the aim of iteratively moving the CINR point closer to the POIs. To make it clear, if the initial distance between the two points is 10 km , with a ratio δ of 0.05, then the aiming point will move iteratively along the line joining the two by 0.5 km each time.

As shown in Figure 5, the subplatform point, POI, and the aiming point are in a straight line. We also assume that the interference at the peak CINR point is much lower than the signal in that region, which means that the peak CINR point will lie close to the same line. According to the figure, the peak CINR point is always at the far side from the subplatform to the POI, so that in order to move the peak CINR point closer to the POI, we should move the aiming point toward to the SPP with each step. We also assume the peak CINR point is close to the straight line containing the aiming point, POI, and SPP.

This scheme can be expressed by the following equation:

$$\overrightarrow{r_{Ai+1}} = (1 + \delta)\overrightarrow{r_{Ai}} - \delta\overrightarrow{r_{Pi}}, \qquad (19)$$

where $\overrightarrow{r_{Ai+1}}$, $\overrightarrow{r_{Ai}}$, $\overrightarrow{r_{Pi}}$ represent the position vector for the different points in the x, y plane, where $\overrightarrow{r_{Ai+1}}$ represents the vector with the symbol.

We repeat the same process at each step (i) which means the generated location in one step will be the condition of next step ($i + 1$) to calculate the new location of the aiming point.

The short step size scheme will not deliver the optimum aiming point after a single stage, so it needs a number of iterations to reach the minimum value. In general, the shorter the step size, the more iterations that are needed to reach the optimum point. However, the scheme moves in a single direction toward the SPP, so it will continue to move the peak CINR beyond the POI after it reaches the minimum point. Therefore, we store the outcome of value after each iteration in order to select the optimum iteration value to minimize the distance between the peak CINR and POI. We assume the optimum mean number of iterations occurs when the distance between the peak CINR and POI is a minimum that is,

$$d_{\min} = \min\left(\text{mean}\left(\left|\overrightarrow{r_{POI\_j}} - \overrightarrow{r_{PCINR\_j}}\right|\right)\right), \qquad (20)$$

where j is the set of beams sharing the same channel.

Figure 6 illustrates the variation of the mean distance value between the POI and peak CINR points with five different coefficients and different iterations from the same antenna beam allocation. This figure shows that the higher value coefficient case requires fewer iterations to reach the mean minimum distance which has the advantage of saving time to finish the antenna positioning. However, the mean minimum distance from the higher value coefficient case tends to be less accurate than the lower ones since it may miss

Max. CINR for configuration of single HAPs point
with the terrestrial systems

(a)

Max. CINR for configuration of single HAPs point
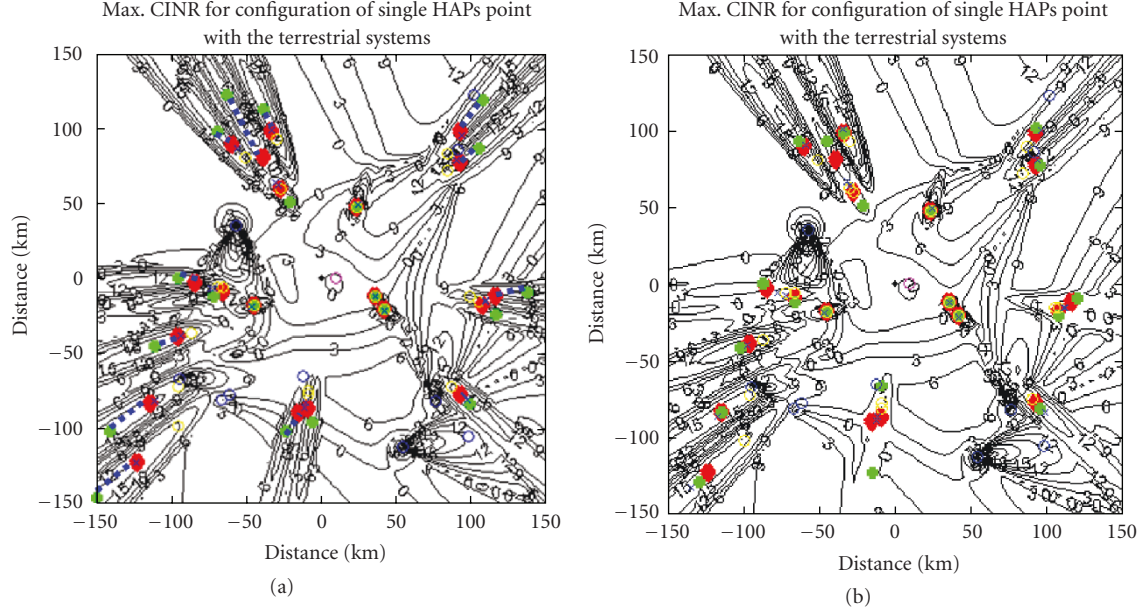with the terrestrial systems

(b)

FIGURE 7: (a) Initial CINR contour plot of single HAP with multiple antenna beams with terrestrial systems. (b) Final CINR contour plot of single HAP with multiple antenna beams with terrestrial systems after applying Scheme I.
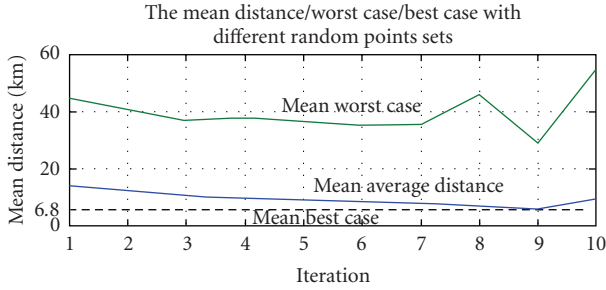
The mean distance/worst case/best case with
different random points sets

FIGURE 8: The mean distance/best case/worst case with different random points sets in small step size scheme.

CDF of mean distance/worst case/best case
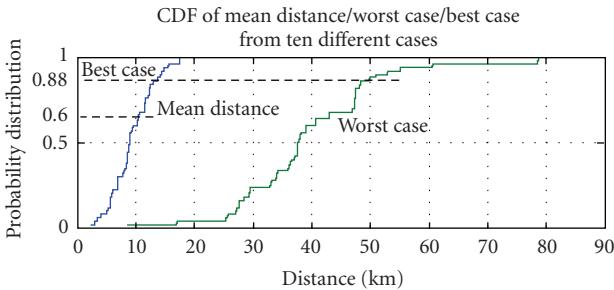from ten different cases

FIGURE 9: The CDF of mean distance/best case/worst case with different random points sets in the small step size scheme.

the minimum point because of the longer step size each time. It clearly illustrates the tradeoff between pointing accuracy and convergence time.

To assess performance, we look at the special effects of the scheme using a contour plot. These are shown in Figure 7.

The green circles represent the peak CINR points, red diamonds represent the POIs, blue circles represent the terrestrial stations, yellow circles specify the aiming points, and the pink circle represents the SPP. As shown in Figure 7, the 0.05 ratio coefficient has been chosen to operate the simulation. The first figure is the initial version of CINR contour and the second one is the modified version, where the positions have been optimized to deliver the best mean CINR at the POIs. Here, the optimum point is reached after 40 iterations. As shown in the figure, most pairs of the peak CINR points and POIs in the first figure initially do not coincide with each other, particularly well outside 50 km radius range. However, after applying the small step size scheme, the pairs of peak CINR point and POI within 50 km coincide even better, and those outside the 50 km range shorten a considerable distance that can be certified in the above figures.

Figure 8 illustrates the mean distance variation between POI and peak CINR for up to 10 iterations. The mean distance drops down smoothly at the beginning, after reaching the minimum point (after 9 iterations) it increases as the peak CINR and POI start to diverge. The minimum value of the mean average distance is 6.8 km according to Figure 8.

Figure 9 shows the CDFs of best, mean, and worst case distances after 20 iterations. It illustrates that 60% of the mean distance cases are within the range of 10 km. For the worst cases, 88% of them are within 50 km. Note that a 50 km distance does not necessarily mean that the CINR is inadequate at the POI, just that it is not a maximum. In any
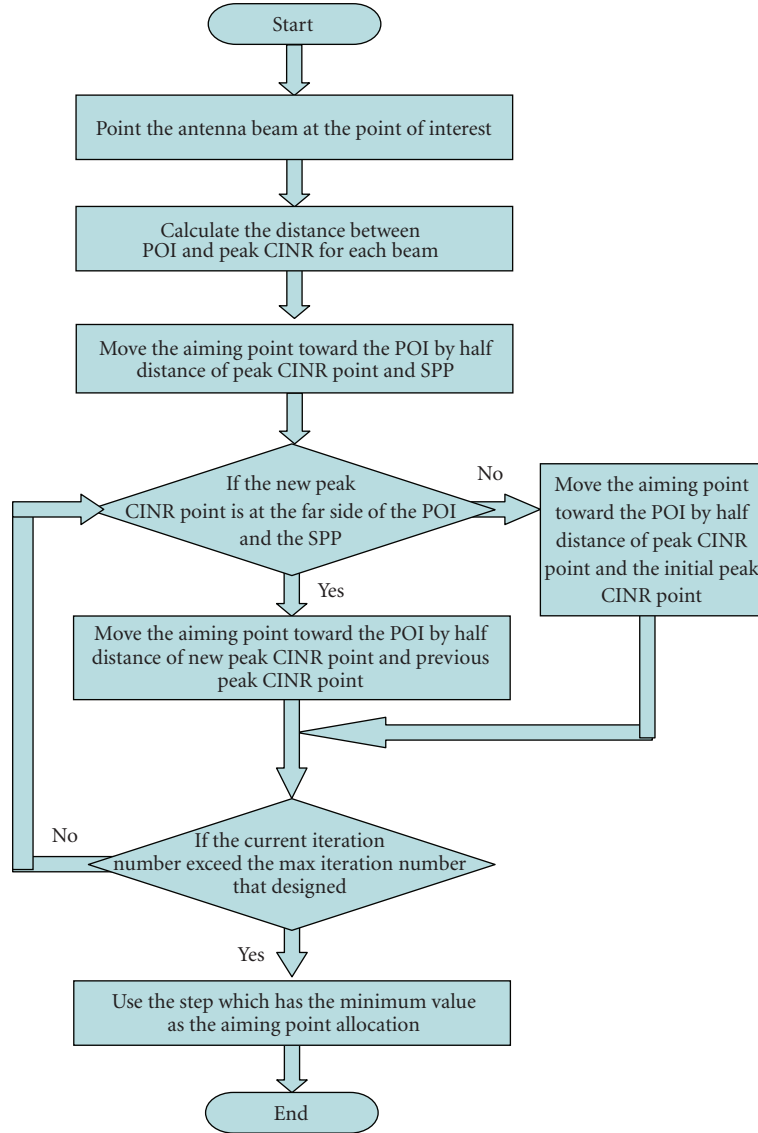
FIGURE 10: The flowchart of the half distance step side scheme.

case, the schemes discussed later show how the peak CINR can be moved closer to the POI.

4.2. Scheme II: half distance step size scheme

The previous scheme moved the aiming point by a short fixed step each iteration and always moved in the same direction toward the SPP, which means that it will deviate from the POI after reaching it, making it difficult to predict the optimum number of iterations. The half distance step size scheme is a creative method to move the peak CINR point to coincide with the POI. This is based on a basic binary search technique. The movement operates similar to the previous scheme, since it still concentrates on moving the aiming point along the line joining the subplatform (SPP) and the POI. However, unlike the short step scheme, we move the aiming point depending on whether the peak

CINR point with the new allocation is between the SPP and the POI or instead outside these two points. The aiming point is iteratively moved each step by half the distance separating the initial or last previous peak CINR point and new peak CINR point, either toward or away from the SPP, depending on the location of the previous position relative to the POI. The mean distance of all peak CINR points and POIs are evaluated each iteration and the process stops after the minimum point has been reached or the maximum number of iterations has occurred. We can see how the half distance scheme works in Figure 10.

The direction of movement is determined by the mutual position of new peak CINR point and POI, however, it always moves toward the POI. To make it clear, we can see how the aiming point changes in Figure 11.

D_1 is defined as the distance between the initial peak CINR point and SPP. Each step, the new location changes to
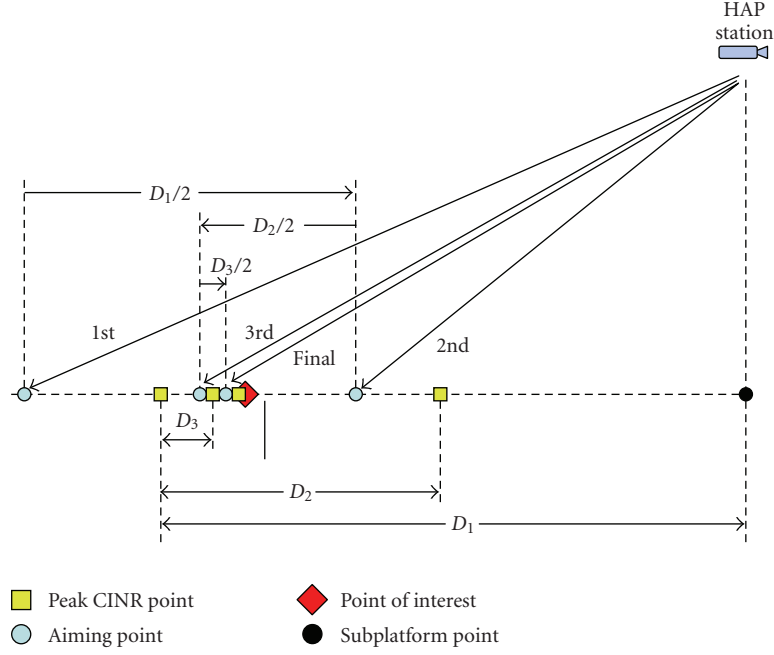
FIGURE 11: The half distance scheme description.

the one between the new peak CINR point and subplatform point (if the new peak CINR point's location is between the POI and SPP) or the one between the initial peak CINR point and new peak CINR point (if the new peak one is between the initial peak CINR point and POI). This scheme ends when the mean distance between peak CINR and POI of all the beams of the previous iteration is less than the current iteration. This scheme is better than Scheme I since it will converge more quickly toward the coordinates of the aiming point.

The scheme can be described by the following equations:
When $-\pi/2 < \arccos(\overrightarrow{POI} \cdot \vec{a_s}/|\overrightarrow{POI}||\vec{a_s}|) \le \pi/2$,

$$\overrightarrow{r_{i+1}} = \begin{cases} \dfrac{\overrightarrow{PC_{i-1}} + \vec{r_i}}{2}, & -\dfrac{\pi}{2} < \arccos\left(\dfrac{\overrightarrow{POI} \cdot \overrightarrow{PCINR}}{|\overrightarrow{POI} \cdot \overrightarrow{PCINR}|}\right) \le \dfrac{\pi}{2}, \\[2ex] \dfrac{\overrightarrow{PC_i} + \vec{r_i}}{2}, & \dfrac{\pi}{2} < \arccos\left(\dfrac{\overrightarrow{POI} \cdot \overrightarrow{PCINR}}{|\overrightarrow{POI} \cdot \overrightarrow{PCINR}|}\right) \le \dfrac{3\pi}{2}, \end{cases}$$

(21)

when $\pi/2 < \arccos(\overrightarrow{POI} \cdot \vec{a_s}/|\overrightarrow{POI}||\vec{a_s}|) \le 3\pi/2$,

$$\overrightarrow{r_{i+1}} = \begin{cases} \dfrac{\overrightarrow{PC_{i-1}} + \vec{r_i}}{2}, & \dfrac{\pi}{2} < \arccos\left(\dfrac{\overrightarrow{POI} \cdot \overrightarrow{PCINR}}{|\overrightarrow{POI} \cdot \overrightarrow{PCINR}|}\right) \le \dfrac{3\pi}{2}, \\[2ex] \dfrac{\overrightarrow{PC_i} + \vec{r_i}}{2}, & -\dfrac{\pi}{2} < \arccos\left(\dfrac{\overrightarrow{POI} \cdot \overrightarrow{PCINR}}{|\overrightarrow{POI} \cdot \overrightarrow{PCINR}|}\right) \le \dfrac{\pi}{2}, \end{cases}$$

(22)

where $\vec{r}$ is the vector of the aiming point, $\vec{a_s}$ is the vector of SPP, $\overrightarrow{POI}$ is the vector of POI, $\overrightarrow{PC_i}$ is the vector of the peak carrier value, and $\overrightarrow{PCINR}$ is the vector of the peak CINR used in the calculation.
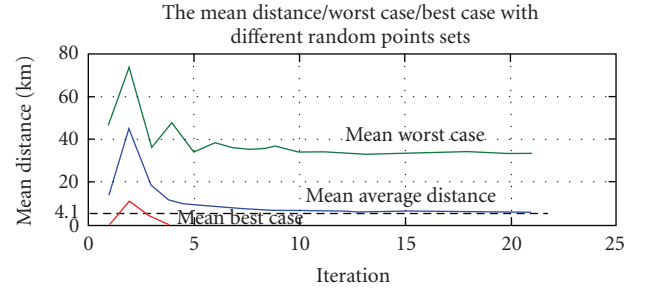

FIGURE 12: The mean distance/best case/worst case with different random points sets in half distance scheme.

In order to compare the mean distance variation with the short step size scheme, this section will show the mean value, worst case, and best case in the simulation process. Figure 12 illustrates the mean distance variation for up to 20 iterations. All the first steps have a very high value due to the initial moving distance being the longest. After a series of fluctuating adjustments, the value becomes stable and appears as the best situation in the process. All the best cases beyond 4 iterations in Figure 12 are equal to zero which means at least one POI receives the highest CINR value, and all the worst cases in Figure 12 distribute between 30 km and 40 km due to the interference from the terrestrial stations and other antenna beams. The minimum value of the mean average distance is 4.1 km which is 2.7 km less than Scheme I. The results from both schemes are based on 100 sets of random points.

Figure 13 shows the CDFs of best, mean, and worst case distances after 20 iterations. It shows that 75% of the mean distance cases are within 10 km on average, with 82% of the
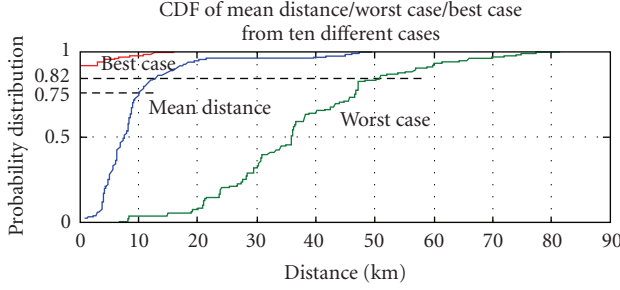
FIGURE 13: The CDF of mean distance/best case/worst case with different random points sets in half distance scheme.
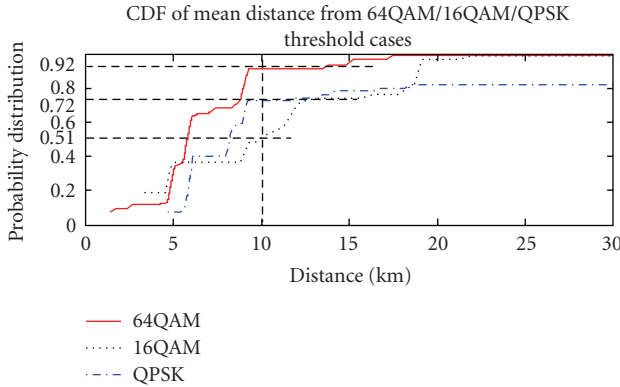

FIGURE 14: CDF plot of mean distance, worst case, and best case from 64 QAM, 16 QAM, and QPSK modulation scheme.

FIGURE 15: Histogram of numbers of beams activated from 64 QAM, 16 QAM, and QPSK modulation scheme.

worst cases being within 50 km. Given the worst case is with a long physical distance, the CINR values at the POIs that they serve are still satisfied under the user's demands. Comparing the mean distance results shows that 75% are below 10 km for Scheme II with 60% for Scheme I. Furthermore, Scheme II normally requires fewer iterations to achieve the same or better minimum mean distance values.

4.3. Scheme III: beam switch off

In this section, we modify Scheme II introduced in the previous section by switching off some of the antenna beams, where the CINR falls below a given level after a set number of iterations, with the aim of reducing the mean distance between peak CINR and POI. In practice, not all the ground users need to be serviced at the same time, and meanwhile the ground users will also require a certain minimum CINR in order to deliver a certain level of service, so such an approach is justified. The first part of the scheme is identical to Scheme II, and it is only when the number of iterations required to reach the minimum value (d_{min}) is confirmed, that the beams failing to meet a predetermined CINR threshold at point of interest are switched off; the CINR is reevaluated. We can see the scheme performance in Figure 14.

We pick three different CINR threshold values to examine their mean distance, worst case, and best case perfor-
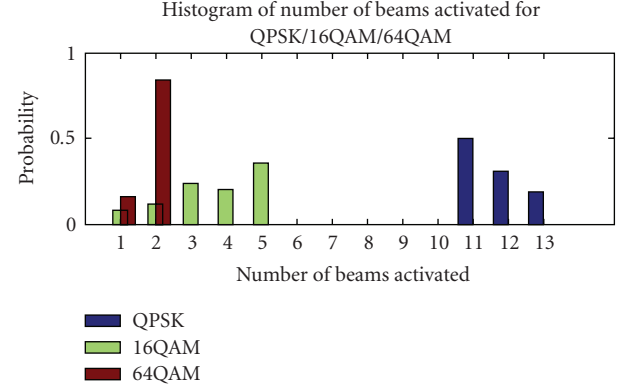
mance. The figure illustrates that the 64QAM with a 20 dB SINR threshold always has the least distance discrepancy, compared with 16QAM with a 16 dB SINR threshold and QPSK with a 7.8 dB SINR threshold cases under all the three circumstances. Using mean distance case as example, 92% of 64QAM cases are within a 10 km range, while the 16QAM and QPSK cases have their respective 72% and 51% within the same distance. Even the worst case 64QAM results offer a solid performance in the 0–90 km range from the center of coverage.

To examine how many beams are still activated after applying the scheme with different modulation rates, we provide a bar chart in Figure 15. The QPSK case normally maintains 11–13 beams when it operates; the 16 QAM can usually operate 1–5 beams, but more commonly there are 3 or 5 beams activated; the 64 QAM modulation scheme has only 1-2 beams, but sometimes only one beam can pass the threshold.

5. CONCLUSION

We have shown how it is possible to use directional antenna beams on an HAP to provide gigabit link communication to the designated specialist user over an extended service area of 300 km diameter. Furthermore, this paper presented a means to accurately direct the peak CINR value to the location of the user under the interference from terrestrial point-to-point systems and other beams on the HAP. It also proposed a technique to further improve performance by switching off the antenna beams which fail a CINR threshold value at the specialist user, in order to improve the CINR at other specialist user locations. We have shown that the number of beams which remain active on the same channel depends on the chosen modulation level at the specialist user. Typically, only 1 or 2 beams can operate with 64QAM, but typically, 11–13 beams remain active with QPSK. Overall, these results indicate that HAP and terrestrial systems can coexist on the same frequency, with the potential to offer gigabit rates to specialist users.

REFERENCES

[1] N. Geri, "Wireless HDTV-compressed or uncompressed? That is the question," AMIMON Ltd, November 2006.

[2] S. R. Lambert, "Legislative Policy Forum on Economic Development," James W Sewall Company, 07DEC06, 2006.

[3] D. Grace, M. H. Capstick, M. Mohorcic, J. Horwath, M. B. Pallavicini, and M. Fitch, "Integrating users into the wider broadband network via high altitude platforms," *IEEE Wireless Communications*, vol. 12, no. 5, pp. 98–105, 2005.

[4] G. M. Djuknic, J. Freidenfelds, and Y. Okunev, "Establishing wireless communications services via high-altitude aeronautical platforms: a concept whose time has come?" *IEEE Communications Magazine*, vol. 35, no. 9, pp. 128–135, 1997.

[5] Recommendation ITU-R F. 1500, "Preferred characteristics of systems in the fixed service using high altitude platform stations operating in the bands 47.2-47.5 GHz and 47.9-48.2 GHz," International Telecommunications Union, 2000.

[6] R. Miura and M. Oodo, "Wireless communications system using stratospheric platforms: R and D program on telecom and broadcasting system using high altitude platform stations," *Journal of the Communications Research Laboratory*, vol. 48, no. 4, pp. 33–48, 2001.

[7] M. Oodo, R. Miura, T. Hori, T. Morisaki, K. Kashiki, and M. Suzuki, "Sharing and compatibility study between fixed service using high altitude platform stations (HAPS) and other services in the 31/28 GHz bands," *Wireless Personal Communications*, vol. 23, no. 1, pp. 3–14, 2002.

[8] J. Thornton, D. Grace, M. H. Capstick, and T. C. Tozer, "Optimizing an array of antennas for cellular coverage from a high altitude platform," *IEEE Transactions on Wireless Communications*, vol. 2, no. 3, pp. 484–492, 2003.

[9] D. Grace, J. Thornton, G. Chen, G. P. White, and T. C. Tozer, "Improving the system capacity of broadband services using multiple high-altitude platforms," *IEEE Transactions on Wireless Communications*, vol. 4, no. 2, pp. 700–709, 2005.

[10] Z. Yang, D. Grace, and P. D. Mitchell, "Downlink performance of WiMAX broadband from high altitude platform and terrestrial deployments sharing a common 3.5 GHz band," in *Proceedings of the IST Mobile Communications Summit*, Dresden, Germany, June 2005.

[11] N. Adatia, B. Watson, and S. Ghosh, "Dual polarized elliptical beam antenna for satellite application," in *Proceedings of the International Symposium on Antennas and Propagation Society*, vol. 19, pp. 488–491, IEEE Press, Piscataway, NJ, USA, June 1981.

[12] J.-M. Park, B.-J. Ku, Y.-S. Kim, and D.-S. Ahn, "Technology development for wireless communications system using stratospheric platform in Korea," in *Proceedings of the 13th IEEE International Symposium on Personal, Indoor and Mobile Radio Communications (PIMRC '02)*, vol. 4, pp. 1577–1581, Lisbon, Portugal, September 2002.